East European Journal of Physics. 1. 101-111 (2025)
DOI:10.26565/2312-4334-2025-1-09 ISSN 2312-4334

INFLUENCE OF THERMAL RADIATION ON MHD CASSON NANOFLUID FLOW OVER A NON-LINEAR STRETCHING SHEET WITH THE PRESENCE OF CHEMICAL REACTION

P. Raja Shekar*, G. Jithender Reddy†, N. Pothanna
Department of Mathematics, VNR Vignana Jyothi Institute of Engineering and Technology, Hyderabad, 500090, Telangana State, India
**Corresponding Author e-mail: rajoct25@gmail.com; †e-mail: jithendergurejala@gmail.com*
Received November 28, 2024; revised January 16, 2025; accepted January 20, 2025

The focus of this research is to examine how the Casson and chemical reaction parameter impact the variable radiative flow of MHD Nanofluid across a stretching sheet. Through the use of similarity functions, the modelling equations (PDEs) of the motion of fluid are transformed into simple differential equations. The MATLAB tool is adopted to compute the equations numerically. Graphs and descriptions have been provided for velocity, concentration, and temperature outlines, showing the effects of important fluid flow constraints. Different factors are analysed to provide data and explanations for Prandtl, Lewis numbers, slip and chemical decomposition parameters. The current results are in good in good align with existed reports. The viscosity of the fluid and thermal boundary stratum decreases as enhancing of Casson, Magnetic parameter & Prandtl number. Skin friction increasing as enhancing of suction, stretching, magnetic and Casson parameter while decreasing as enhancing of velocity slip quantity. Rate of heat transmission enhancing as increment of thermal radiation and surface temperature while decreasing as enhancing chemical reaction and thermal slip quantities. Rate of mass transfer raising as enhancing of chemical reaction, thermal slip, thermal radiation while decreasing as enhancing of surface temperature parameter.
Keywords: *Nanofluid; Chemical reaction; Thermophoresis; Brownian Motion*
PACS: 47.10.A−, 44.40.+a, 47.11.−j, 52.65.Kj

INTRODUCTION

Boundary stratum flow on a stretched sheet is a noteworthy problem in different industrial developments like paper manufacturing and drawing plastic, glass, fiber & elasticity sheets. This phenomenon can also be observed in the growth of crystals during polymer stretching processes and the cooling of metal sheets in cooling baths. Scientists are focusing on this issue because of its relevance in polymer processing technology, especially in relation to heat transfer applications. Sakiadis [1] made significant contributions to this area by investigating the equations controlling the boundary stratum and flow over an expanding surface moving at a constant velocity. Elbashbeshy and Bazid [2] explored the flow of fluids and heat transmission on a newly explored extended surface by internal heat activation given the importance of these phenomena. Several scholars further developed Crane's work [3] done through the influence of heat & mass transfer by different geometries & shapes, as explored by Abbas et al. [4] and Rosca et al [5].

Base fluids including water, motor oil, and glycerin combined with scattered nanoparticles like carbon nanotubes, copper, silver, and gold make up nanofluid. The idea of utilizing a nanofluid, which is a mixture of a base fluid & nano sized particles, was initially proposed by Choi and Eastman [6]. Solid particles are evenly and durably spread out in the base liquid, such as water, engine oil, pump oil, and ethylene glycol. Nanofluid's are predicted towards the next future of heat transmission fluids because of their ability to greatly improve heat transfer efficiency when compared to pure liquids. Their excellent thermal, chemical, and physical characteristics are highly useful in various industrial and technological applications. Moreover, nanofluids have the potential to enhance abrasion characteristics in comparison with traditional fluid blends. The scattered nanoparticles, often metals or metal oxides, enhance the thermal diffusion of nanofluid's. A variety of thermal applications, including smart fluids, microelectronics, heat exchangers, fuel cells, hybrid-powered generators, pharmaceutical manufacturing, nuclear reactors, industrial cooling, and geothermal power extraction, can benefit from the unique properties of nanofluids. Various researchers have recently finished several studies on nanofluids. Das [7] investigated the behaviour of heat & mass transfer in MHD nanofluid flow across a radiating non-linear permeable extending sheet with changes in thermal & velocity slip. He and his colleagues used the 4th order RK-Fehlberg method along through the shooting method procedure to calculate computational solutions for modelling equations Entropy was investigated by Hayat et al. [8] in a radiative water-based nanofluid between two rotating disks. Wang et al. [9] conducted a computational evaluation of microchannel porous materials by introducing two distinct nanoparticles into a base fluid. Khan and Pop [10] examined nanofluid flow on a flat surface undergoing stretching with Brownian and thermophoresis using an implicit finite-difference method.

In recent years, investigating and describing the advanced properties of composite flows has become a fundamental focus of research. The area of research involving conductive liquids that exhibit magnetic field characteristics is known as magnetohydrodynamics (MHD). Rahman and Eltayeb [11] conducted a computational study on the properties of heat transmission of nanofluid's flowing over a non-linear extending sheet in two dimensions under hydromagnetic natural convection. The study used the mathematical computer program Maple, accounting for the effects of thermal radiation

Cite as: P.R. Shekar, G.J. Reddy, N. Pothanna, East Eur. J. Phys. 1, 101 (2025), https://doi.org/10.26565/2312-4334-2025-1-09

and a convective frontier circumstance. Tausif et al. [12] studied the influence of a magnetic field on nanofluid flow across a non-linear permeable extending sheet boundary layer. Mahantesh et al.'s [13] investigation of MHD fluid flow as well as heat transmission at a point of stagnation took into account non-uniform heating source and sink effects, slip velocity, and thermal leap. The results were reported numerically. Using a two-term perturbation approach, Vedavathi et al. [14] discovered MHD nanofluid circulation on a flat plate while taking radiation absorption, diffusion thermodynamics, and first-order chemical reactions into account. Biswas et al. [15] researched a concentrated nano liquid model over a perpendicular plate. Moreover, in order to finish the project, they utilized an explicit finite difference approach to visually analyse the temperature, concentration, and velocity profiles. Beg et al. [16] examined nanomaterial flow with mixed convection through porous space that starts from an exponentially stretched sheet. However, Al-Mamun et al. [17] inspected the flow of Sisko-nanofluid across an extended nonlinear sheet, taking into the consideration of thermal radiation & the magnetohydrodynamic (MHD) effect. The effects of ion-slip and Hall current on transient magnetohydrodynamic (MHD) flow in a revolving porous medium were studied by Dharmaiah et al. [18]. In a magnetohydrodynamic convective micropolar fluid moving steadily over an inclined radioactive isothermal surface, the interaction amid thermophoresis and heat production and absorption was examined by Shaik Mohammed et al. [19].

Casson fluid, a significant non-Newtonian liquid, is increasingly crucial in our daily lives. Different kinds of sauces, soups & jellies illustrate Casson fluids. In 1959, Casson [20] was the first to develop the modelling equations for Casson fluid and demonstrate the characteristics of different polymers. McDonald [21] highlighted that, the Casson liquid model is characterized by the flow of blood. The class of fluids being discussed has a broad variety of uses in medicine, food industries, biological sciences, and various drilling processes. Because of its significant relevance, numerous researchers in the modern era observe this critical category of fluids in their laboratories. Nagarani et al [22] investigated the movement of Casson liquid in tube with supple ramparts and the spread of solute using peristaltic flow. Vishwanath et al. [23] analyzed the magnetohydrodynamic (MHD) movement of Casson fluid, which is non-Newtonian, on a surface that shrinks exponentially. The surface had both constant and exponentially changing wall temperature with suction. The dynamic behaviour of modelled equations, explaining the motion of micropolar Casson fluid across a sheet was inspected by Nadeem and colleagues [24] with exponential curvature. In their study, Narsimha Reddy and colleagues [25] examined the impact The nanofluid Casson and joules parameter in the varying radiative flow of a stretched sheet with MHD. Reddy and colleagues [26] investigated the flow of a Casson incompressible fluid with heat generation and magnetic field, driven by mixed convective, on a vertically accelerating porous plate.

Among the most crucial process variables for heat & fluid transport in a high temperature thermal system is radiation characteristics. There are several applications for thermal energy in industries as a means of reducing excessive heat emission. One important factor influencing the growth of nuclear energy, steady kit, turbines of gas, satellites, assortment of innovative transformation structures and missiles facilities is thermal radiation, For the determination of analyzing the MHD H_2O-based nanofluid with the effects of significant variables on heat transmission & liquid movement characteristics are inspected by Dharmendra et al. [27]. Nurul et al. [28] highlighted hybrid nanofluids by modelling stagnation point flow in Maxwell fluid. They also studied heat transfer and radiation effects. Analysis of the implications of mixed convection, thermal radiation, and porous media were considered by Abdul Wahed et al. [29]. The goal of Rashad et al.'s work [30] was to develop a computational framework for the MHD Eyring–Powell nanofluid hybrid mixed convection flux when thermal radiation is present. The nano liquid flow between two horizontally infinite plates with a stretchable and permeability lower plate was deliberated by Shaheen [31]. Arulmozhi et al. [32] compare the effects of pure fluid (water) and nanofluid (Cu–H2O) on a moving vertical plate with porosity. By taking into account the nanoparticles' ability to reach thermal equilibrium, the chemical response of this nanofluid with regard to radiation absorption is consider. The effects of radiation and chemical responses on MHD hyperbolic tangent liquid were studied by Athal et al. [33]. The combined effects of radiative heat, thermophoresis, mixed convective heat, Brownian motion, and chemically reactive species were deliberated by Ahmed [34] in relation to magnetohydrodynamic (MHD) flow through the frontier stratum of nanofluid across a non-linear extending a porous medium surface. In the incidence of reactive chemical species and Joule heating, the simultaneous impacts of radiation on the convection of MHD nanofluid across an extensible sheet in permeable medium were examined by Eid and Makinde [35]. Eldabe et al. [36] described the influence of a chemical response on the MHD frontier stratum of an Eyring Powell nanofluid flowing with heat transmission through an extended sheet. Gireesha1 and N. G. Rudraswamy [37] have investigated the effects of chemical processes on stagnation point movement along with heat transmission over an extensible surface of a nano liquid in the incidence of irregular heat source/sink & uniform magnetic field. Anupam Bhandari [38] investigated the stable state of a 2-dimensional incompressible flow of MHD with a micropolar nanofluid across an extended sheet.

Comprehending how nanofluids behave in linear and non-linear stretching situations is important for a range of applications, such as industrial processes, coating applications, material manufacturing, and biomedical uses [39-40]. Investigations in this field help in the comprehension of how nanofluid impact the flow & heat transfer attributes in diverse extending situations, offering valuable information for use in a range of industries. This study addresses various gaps and limitations found in the previously discussed literature. It aims to develop a scientific model to inspect the possessions of radiation on MHD Casson nanofluid movement on a nonlinear extending sheet, incorporating surface temperature & concentration. The inclusion of thermal radiation adds novelty to the problem. The flow is examined under the influence of a nonlinear extending sheet in the existence of a chemical response. This model has practical applications

in areas such as nuclear waste storage, catalytic devices, fire-resistant insulation, & the production of pharmaceuticals, painting, coal-water mixtures and synthetic lubricants.

MATHEMATICAL FORMULATION

The study focused on a non-Newtonian nanofluid movement across an extending surface sheet with a nonlinear boundary layer at the plane $y = 0$. Flow is limited when $y > 0$, with the y axis vertical to the sheet described in Figure 1. It is presumed that the plate is extending along the $x-$ direction, consider a non-linear velocity $u_w = ax^n, a > 0$ $-$ direction where a >0 is a constant number, n is the extending parameter that varies nonlinearly, and x is the co-ordinate along the extending surface. The applied magnetic field $B(x)$ normal to the extending sheet causes the fluid to become electrically conductive, with B_0 being the initial intensity of the field of magnetism. The temperature on the stretching sheet at y=0 is given by $T_w = T_\infty + bx^r$ where the temperature far from the surface is denoted by T_∞ , the surface temperature parameter (STP) is represented by r, and b is a constant that is positive By setting r=0 in certain scenarios, we achieve a consistent temperature across the sheet, known as constant surface temperature (CST). C represents the concentration of nanoparticles, while C_w is the consistent concentration of nanoparticles on the plate's surface, which is higher than the surrounding fluid concentration C_∞ . Additionally, the magnetic Reynolds number is extremely low and can be ignored, resulting in a small induced magnetic field.

The Cauchy stress tensor rheological equation for Casson nanofluid is provided.

$$\tau' = \tau_0 + \mu\gamma \text{ Or } \tau_{ij} = \begin{cases} 2\left(\mu_B + \dfrac{p_y}{\sqrt{2\pi}}\right)e_{ij}, & \pi > \pi_c \\ 2\left(\mu_B + \dfrac{p_y}{\sqrt{2\pi_c}}\right)e_{ij}, & \pi > \pi_c \end{cases}$$

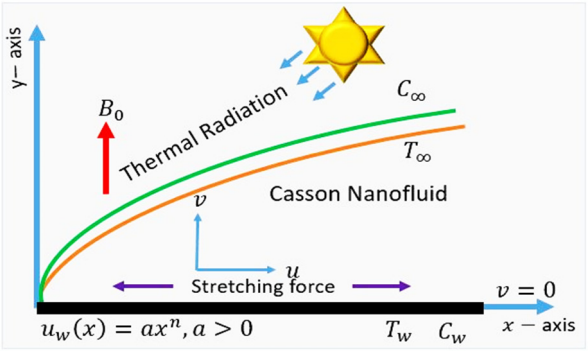

Figure 1. Geometric and physical representation model

In view of the overhead norms and considerations, the PDE models for nanofluid flow in the laminar boundary layer are derived.

$$\frac{\partial u}{\partial x} + \frac{\partial v}{\partial y} = 0, \tag{1}$$

$$u\frac{\partial u}{\partial x} + v\frac{\partial v}{\partial y} = v\left(1 + \frac{1}{\gamma}\right)\frac{\partial^2 u}{\partial y^2} + \frac{\sigma B(x)^2}{\rho_f}u, \tag{2}$$

$$u\frac{\partial T}{\partial x} + v\frac{\partial T}{\partial y} = \alpha\frac{\partial^2 u}{\partial y^2} + \tau\left\{D_B\left(\frac{\partial C}{\partial y}\frac{\partial T}{\partial y}\right)u + \frac{D_T}{T_\infty}\left(\frac{\partial T}{\partial y}\right)^2\right\} - \frac{1}{\rho c_p}\frac{\partial q_r}{\partial y}, \tag{3}$$

$$u\frac{\partial C}{\partial x} + v\frac{\partial C}{\partial y} = D_B\frac{\partial^2 C}{\partial y^2} + \frac{D_T}{T_\infty}\frac{\partial^2 T}{\partial y^2} - k_0(C - C_\infty). \tag{4}$$

Subject to the slip boundary conditions

With boundary condition

$$\left.\begin{array}{c} u = u_s + u_w, v = v_w, T = T_s + T_w, C = C_w \text{ for } y = 0 \\ u = 0, v = 0, T = T_\infty, C = C_\infty \text{ as } y \to \infty \end{array}\right\}. \tag{5}$$

Where u and v are velocity along x and y directions. u_s and T_s are the velocity & thermal slip, v_w is suction or injection, ρ_f is density of the base liquid, σ is electrical conductivity, , ν is kinematic viscosity and $\alpha = \frac{\kappa}{(\rho c)_f}$ is thermal diffusivity of the base liquid. D_B and D_T are Brownian & thermophoretic diffusion constants correspondingly, c_p is the specific heat, k_0 is rate of chemical reaction, $B(x) = B_0 x^{(n-1)/2}$ variable magnetic field, $\tau = \frac{(\rho c)_p}{(\rho c)_f}$ is the ratio of the heat capacity of

the nanoparticles to heat capacity of the base fluid. C is concentration of nanoparticles, C_w is consistent concentration of nanoparticles at surface, greater than the ambient concentration C_∞ .

If we consider an optical thick frontier stratum where the Rosseland estimation, the radioactive heat flux q_r becomes

$$q_r = -\frac{4\ddot{\sigma}}{3\ddot{\kappa}}\frac{\partial T^4}{\partial y}, \tag{6}$$

where $\ddot{\sigma}$ & $\ddot{\kappa}$ are the Stephan–Boltzmann & mean absorption coefficients.
Replacing Eq. (6) in the leading Eq. (3) we get

$$u\frac{\partial T}{\partial x} + v\frac{\partial T}{\partial y} = \alpha\frac{\partial^2 u}{\partial y^2} + \tau\left\{D_B\left(\frac{\partial C}{\partial y}\frac{\partial T}{\partial y}\right)u + \frac{D_T}{T_\infty}\left(\frac{\partial T}{\partial y}\right)^2\right\} + \frac{\nu}{C_p}\left(\frac{\partial u}{\partial y}\right)^2 + \frac{4\ddot{\sigma}}{3\ddot{\kappa}\rho c_p}\frac{\partial}{\partial y}\left(T^3\frac{\partial T^3}{\partial y}\right). \tag{7}$$

The dimensionless measures as

$$\eta = y\sqrt{\frac{a(n+1)}{2\nu}}x^{\frac{n-1}{2}}, u = ax^n f'(\eta), v = \sqrt{\frac{a\nu(n+1)}{2\nu}}x^{\frac{n-1}{2}}\left(f(\eta) + \frac{n-1}{n+1}\eta f'(\eta)\right), \theta(\eta) = \frac{\mathrm{T}-\mathrm{T}_\infty}{\mathrm{T}_w-\mathrm{T}_\infty}, \varphi(\eta) = \frac{\mathrm{C}-\mathrm{C}_\infty}{\mathrm{C}_w-\mathrm{C}_\infty}, \tag{8}$$

here $\psi(x, y)$ is stream function defined by

$$u = \frac{\partial\psi}{\partial y} \text{ and } v = \frac{\partial\psi}{\partial x}. \tag{9}$$

These are satisfying the Eq. (1) and the equations (2)-(5), obtained the equations (10)-(13) as follows

$$\left(1+\frac{1}{\gamma}\right)f''' + ff'' - \left(\frac{2n}{n+1}\right)f'^2 - Mf' = 0 \tag{10}$$

$$\theta'' + Pr\left(f\theta' + Nb\varphi'\theta' + Nt\theta'^2 - \left(\frac{2r}{n+1}\right)f'\theta\right) + \left(\frac{4Pr}{3R}\right)[\{1+(T_r-1)\theta\}^3\theta']' = 0 \tag{11}$$

$$\varphi'' + Lef\varphi' + \frac{Nt}{Nb}\theta'' - krLe\varphi = 0 \tag{12}$$

With boundary conditions as

$$\left.\begin{array}{c} f(0) = f_w,\ f'(0) = 1 + \xi f''(0), \theta'(0) = 1 + \zeta\theta', \varphi(0) = 1 \\ f'(\infty) = 0, \theta(\infty) = 0, \varphi(\infty) = 0 \end{array}\right\}. \tag{13}$$

Here, the dash indicates the derivative with η. f, θ, φ are the similarity function, non-dimensional temperature & concentration of nanoparticle respectively, $Pr = \frac{\nu}{\alpha}, Le = \frac{\nu}{D_B}$ are Prandtl and Lewis number respectively. $Nb = \frac{(\rho c)_p}{(\rho c)_f}\frac{D_B(C_w-C_\infty)}{\nu}$, $= \frac{(\rho c)_p}{(\rho c)_f}\frac{D_T(T_w-T_\infty)}{\nu T_\infty}$, $kr = \frac{k_0\nu}{a^2}$ and $M = \frac{2\sigma B_0^2}{a\rho_f(n+1)}$ are Brownian motion, thermophoresis, Chemical and Magnetic parameters respectively. The parameter for fluid's comparative ratio of temperature at the sheet's surface is $T_r = \frac{T_w}{T_\infty}$, $f_w = v_0\sqrt{\frac{2}{a\nu(n+1)}}$ is suction or injuction, $\xi = s_v\sqrt{\frac{a(n+1)}{2\nu}}$ and $\zeta = s_t\sqrt{\frac{a(n+1)}{2\nu}}$ are the velocity & thermal slips respectively where s_v ands_t are the velocity and thermal factors, The measures of the physical importance are the local skin friction coefficient C_{fx}, the local Nusselt number Nu_x and the local Sherwood number Sh_x which are defined as . $f_w = 0, f_w > 0$, $f_w < 0$ are represents surface is impermeable, suction and injection of the fluid on a porous sheet respectively.

The physical interest's quantities, which are essential for practical reasons

$$C_{fx} = \frac{\mu_f}{\rho U_w^2}\left(\frac{\partial u}{\partial y}\right)_{y=0}, Nu_x = \frac{q_w}{\kappa(T_f-T_\infty)}\left(\frac{4Pr}{3R}\right)[\{1+(T_r-1)\theta\}^3\theta']', Sh_x = \frac{xq_m}{D_B(C_w-C_\infty)}.$$

Where q_w and q_m are the heat and mass flux at the surface, κ is the thermal conductivity of the nanofluid, respectively. The q_w and q_m are given by

$$q_w = -\left(\frac{\partial T}{\partial y}\right)_{y=0} \text{ and } q_w = -D_B\left(\frac{\partial C}{\partial y}\right)_{y=0}$$

The non-dimensional forms of the skin friction, the local Nusselt & the local Sherwood numbers as

$$Re_x^{1/2}C_{fx} = \left(1+\frac{1}{\gamma}\right)f''(0), \frac{Nu_x}{Re_x^{1/2}} = -\left[1+\frac{4}{3R}\{1+(T_r-1)\theta(0)\}^3\right]\theta'(0), \frac{Sh_x}{Re_x^{1/2}} = -\varphi'(0)$$

where $Re_x = xu_w/\nu$ is the local Reynolds number.

DISCUSSION OF FINDING

To calculate the numerical solutions to (10)–(12) with boundary conditions (13), the authors used bvp4c. One of MATLAB's built-in function bvp4c for working with finite difference and collocation polynomials. This technique gives

good agreement results to the other methods which is shown in the Table 1. Numerical calculations are conducted in this part for various parameter values that reflect the flow characteristics, and the outcomes are visually represented.

Code of Validation: Comparison of Nusselt number & Sherwood number tabulated below. The present model is similar of Khan and Pop [10], Rahman and Eltayeb [11] and Das et al [7] when the absence of magnetic, thermal radiation, stretching, suction and surface temperature, Casson and chemical reaction parameters. The present results are good alignment with existed studies by Finite difference (Khan and Pop [10]), Maple software (Rahman and Eltayeb [11]), and RK-Fehlberg method with a shooting method (Das et al [7].

Table 1. The Nusselt and the Sherwood number comparison when $Pr = 2, Le = 2, \eta_\infty = 6$

Nt	**Khan and Pop [10]**		**Rahman and Eltayeb [11]**		**Das et al [7]**		**Present Results**	
	$\boldsymbol{\theta'(0)}$	$\boldsymbol{\varphi'(0)}$	$\boldsymbol{\theta'(0)}$	$\boldsymbol{\varphi'(0)}$	$\boldsymbol{\theta'(0)}$	$\boldsymbol{\varphi'(0)}$	$\boldsymbol{\theta'(0)}$	$\boldsymbol{\varphi'(0)}$
0.1	0.9524	2.1294	0.952376	2.129393	0.95237602	2.12939273	0.95233794	2.12909712
0.2	0.6932	2.2740	0.693174	2.274020	0.69315023	2.27402065	0.69316392	2.27352695
0.3	0.5201	2.5286	0.520079	2.528636	0.52001607	2.52863590	0.52009015	2.52790541
0.4	0.4026	2.7952	0.402581	2.795167	0.40258040	2.79516710	0.40260786	2.79417165

The influence of the Casson fluid parameter (γ) on the velocity outline is portrayed in Figure 2(a). The Casson parameter γ is noted for generating a resistive force in liquid movement. As a consequence, the velocity profile decreases in magnitude with increased values of γ. Increasing γ results in a stronger impact on the temperature field (figure 2(b)). The thickness of the concentration boundary layer will raise as the values of γ increase. The retarding force caused by plastic viscosity contributes to the increased concentration shown in Figure 2(c).

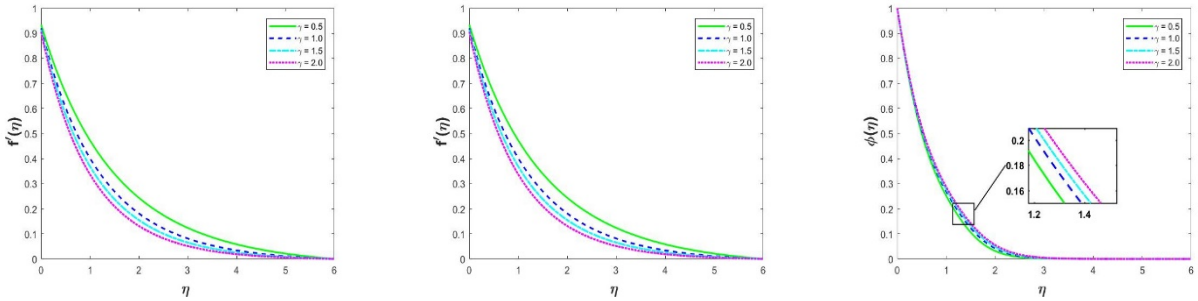

(a) (b) (c)

Figure 2. Impact of Casson parameter on (a) Velocity, (b) Temperature (c) Concentration

The presence of a magnetic field factor leads to an increased distribution of nanoparticles in the boundary layer area. This event is caused by the Lorentz force, which creates a force that goes against the path of fluid movement. Figure 3(b) shows by what means the temperature outlines change with the magnetic field parameter M. It is clear that as M increases, the fluid temperature also increases. The magnetic field makes the magnetic nanoparticles in the nanofluid move and rotate. The drive of the nanoparticles creates friction and crashes, resulting in a rise in temperature by transforming kinetic energy into thermal energy. Additionally, the electrically conducting nanofluid experiences a Lorentz force owing to the functional magnetic field. This energy causes electrical power to transform into warmth, causing the fluid's temperature to rise overall. Therefore, as the magnetic parameter M increases, the thermal boundary layer thickness also increases.

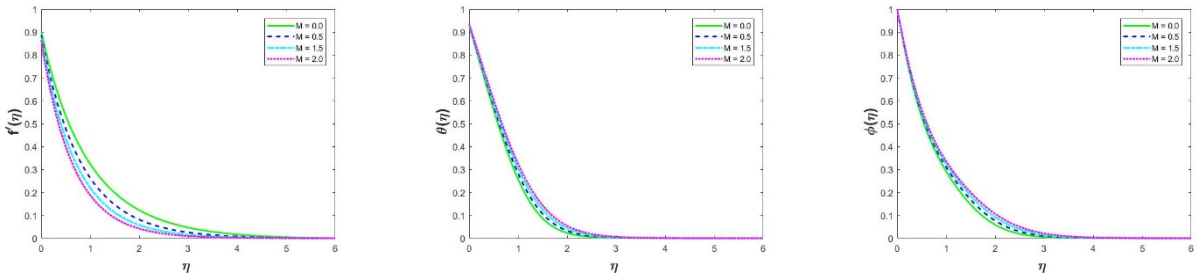

(a) (b) (c)

Figure 3. Impact of M on (a) Velocity, (b) Temperature (c) Concentration

Figure 4(a) demonstrates how the stream-wise velocity varies with different values of the non-linearly stretching sheet parameter n. An increase in this non-linear factor is linked to a decrease in the velocity in the direction of the stream. This suggests that either the stretching process or the parameterization conditions are instigating a deceleration in the movement in the flow path. Consequently, when the parameter n increases, the boundary layer width of impetus decreases. In Figure 4(b), the correlation among temperature variation and parameter n values is illustrated. A greater stretching parameter value means a stronger or more notable extending of the surface. When the surface is stretched more, it adds

extra energy to the fluid movement close to the surface. This extending accomplishment can change the flow outlines, impacting the speed circulation within the boundary sheet. This increases the transmission of momentum and movement of fluids close to the surface, resulting in a thicker boundary layer. Figure 4 illustrates how the nanoparticle concentration profile fluctuations vary with different stretching parameter values, denoted as n. While the effect may be minimal at a constant surface temperature, it is evident that the concentration upsurges as the stretching parameter values upsurge. This happens because the stretching movement can cause improved blending, heightened fluid movement, and changed velocity patterns near the stretched area. This results in increased shear forces in the fluid close to the extended surface. Increased shear stresses improve fluid mixing, resulting in greater transport of species, like substance concentration.

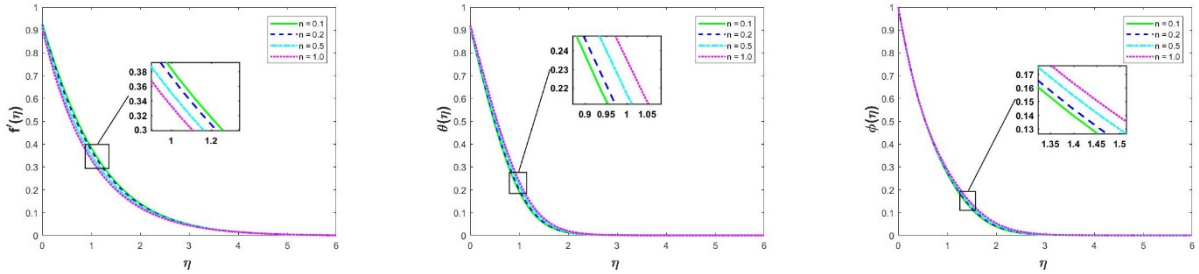

(a) (b) (c)

Figure 4. Impact of n on (a) Velocity, (b) Temperature (c) Concentration

The illustration of how velocity contours behave with dissimilar values of velocity slip parameter ($\boldsymbol{\xi}$) is demonstrated in Fig. 5(a). In general, $\boldsymbol{\xi}$ computes the amount of slip on the cylinder's surface. In this analysis, we examine how fluid speed diminutions with cumulative $\boldsymbol{\xi}$. The cause for this is that $\boldsymbol{\xi}$ primarily hinders the flow of the liquid, which ultimately outcomes in a reduction in overall fluid molecule movement. As the value of $\boldsymbol{\xi}$ increases, it is noted that the concentration and temperature also increase.

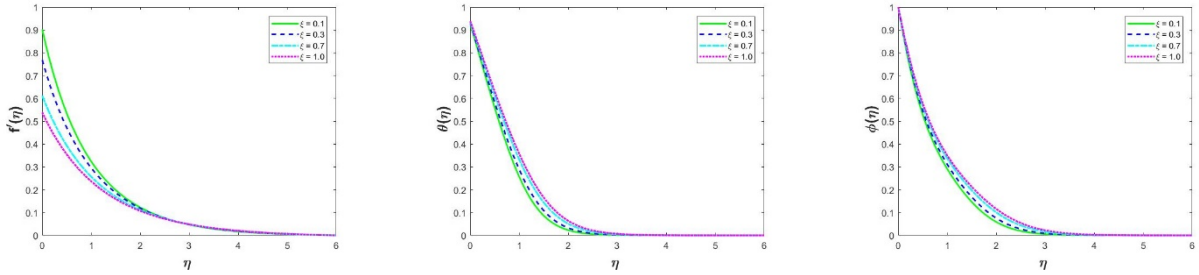

(a) (b) (c)

Figure 5. Impact of velocity slip ξ on (a) Velocity, (b) Temperature (c) Concentration

Figure 6(a) and (b) illustrate how the dimensionless temperature and nanoparticle volume fraction are prejudiced by the thermal slip parameter $\boldsymbol{\zeta}$. Increasing $\boldsymbol{\zeta}$ values clearly reduce temperature and concentration profiles. Even with a modest quantity of heat supplied to the liquid from the sheet, the thermal boundary layer thickness falls with growing thermal slip parameter.

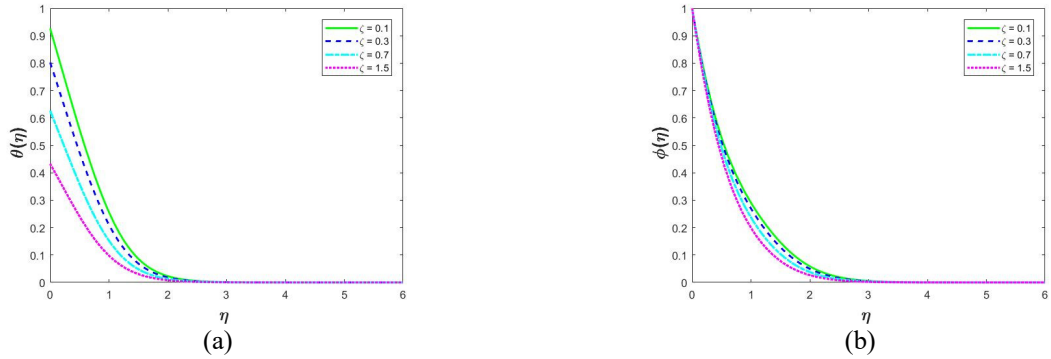

(a) (b)

Figure 6. Impact of thermal slip ζ on (a) Temperature (b) Concentration

Fig. 7(a) shows that the temperature drops with an upsurge in the Prandtl number (Pr). An elevation in Pr could potentially decrease the thermal boundary layer thickness. Pr is the fraction of momentum diffusivity to thermal diffusivity. When dealing with heat transmission matters, the Pr number influences the proportionate growth of the momentum & thermal frontier stratums. When Pr is low, heat spreads rapidly relative to momentum in liquid metals,

resulting in a thermal boundary layer thickness significantly larger than the momentum boundary layer. Liquids with a lesser Pr number exhibit increased thermal conductivities (and thicker frontier stratum structures), allowing for quicker heat diffusion compared to fluids with greater Pr numbers (resulting in thinner frontier stratums) Figure 7(b). Therefore, Pr can be utilized to enhance the rate of cooling in conductive flows.

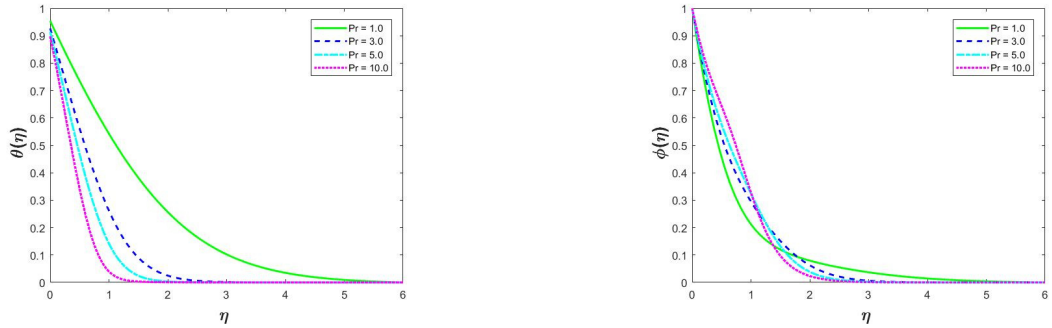

Figure 7. Impact of Pr on (a) Temperature (b) Concentration

Figures 8(a) and 8(b) show how temperature and concentration change with coordinate η for different thermophoretic parameter (Nt) values. The force Nt is caused by the temperature variance among the cold sheet and the hot fluid, leading molecules to move towards the cold sheet. The molecules near the hot stretching sheet are kept warm by the air molecules, resulting in a rapid flow away from the sheet that reduces the temperature difference. This leads to molecules increasing their kinetic energy and temperature. Consequently, the thermophoresis force moved the heated molecules close to the heated contracting surface towards the cold fluid at the surrounding temperature. Thermophoresis causes the momentum boundary layer width to increase, while at the same time thickening the thermal boundary layer width. Graph 8(b) indicates that nanoparticle concentration rises as the thermophoresis parameter increases. Essentially, when a particle exerts a thermophoresis force on another particle, it causes particles to move from a hotter to a colder area, resulting in the fluid moving from a hotter to a colder region, causing the volume proportion of nanoparticles to increase.

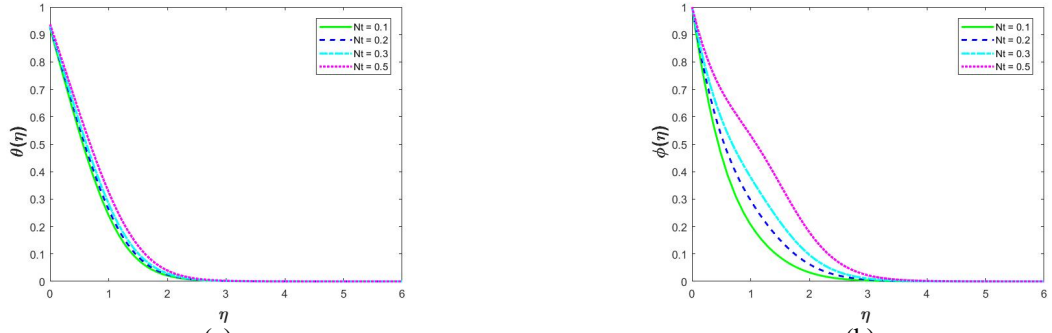

Figure 8. Impact of Nt on (a) Temperature (b) Concentration

The influence of the Brownian diffusion parameter (Nb) on the dimensionless temperature & concentration distributions is demonstrated in Figs 9(a) and 9(b). Brownian diffusion involves the unpredictable movement of nanoparticles suspended in the base liquid, mainly due to the rapid movement of atoms or molecules in the base fluid. It should be noted that Brownian diffusion is connected to the dimensions of nano-particles and frequently appear as clusters and/or clumps. Brownian motion is significantly reduced for larger particles, resulting in Nb having minimal values. As the Nb values increase, the temperature outlines in the frontier stratum region are enhanced (Fig. 9(a)). Nevertheless, the nano particle concentration patterns slow down with increased values of Nb depicted in Fig. 9(b).

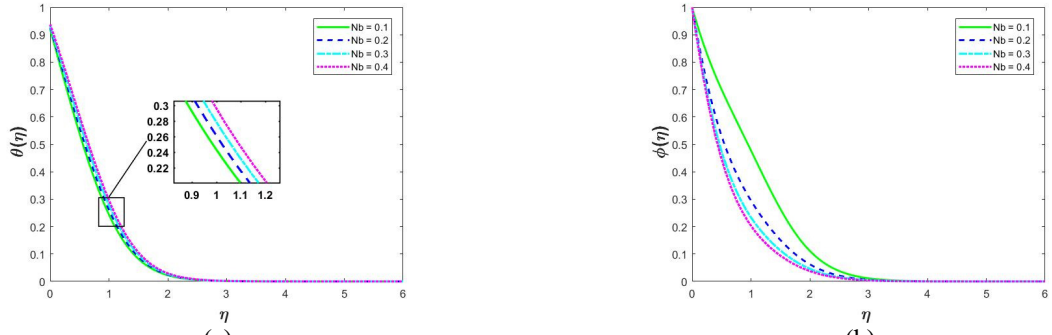

Figure 9. Impact of Nb on (a) Temperature (b) Concentration

Fig. 10(a) displays the temperature distribution for various radiation factor (R) values. It was found that as the R increased, the temperature rose as well. The temperature increased because of the escalation in the conduction effect inside the thermal frontier stratum caused by the rise in R, since the radiation factor was the fraction of conductive heat transfer to radiative heat transfer. This finding may prove useful in directing the ratio of heat transfer properties by means of the thermal radiation mechanism. Fig. 10(b) makes it apparent that when the radiation rises, the fluid's concentration falls.

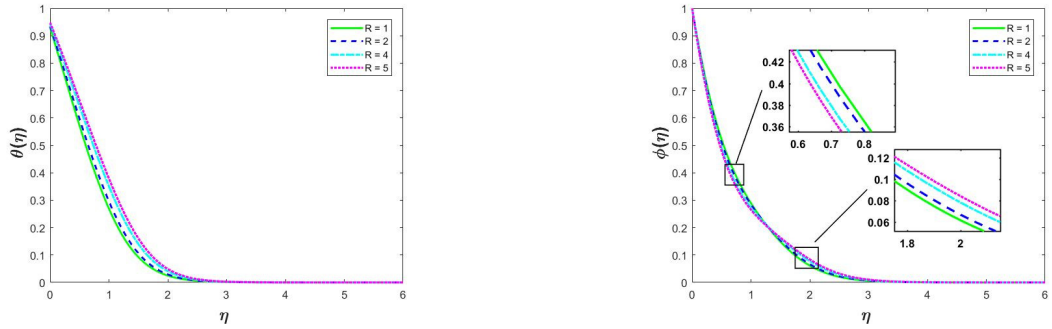

Figure 10. Impact of R on (a) Temperature (b) Concentration

The Lewis number is a unit less parameter that represents the proportion of thermal diffusivity to mass diffusivity and is crucial in the joint impact of heat & mass transfer operations. The relative thermal and concentration boundary layer thicknesses are measured by Le and can also be written as $Le = Sc/Pr$. Reportedly, as Le increases, the temperature decreases sources a lessening in the thickness of the boundary layer fluid. A growth in the parameter slowly enables the fluid to release heat to the external environment or nearby body, resulting in a diminution in the fluid's temperature (Figure 11(a)). Figure 11(b) illustrates how the nanoparticle concentration falls as the Lewis Number (Le) rises. This impact is especially noticeable for smaller Le values. As a result, it is expected that Le will greatly change the concentration frontier stratum. In Figure 12(a) and 12(b), we can see the dimensionless temperature and concentration profile at various values of chemical response. The fluid temperature & concentration declines as the chemical reaction rate rises. The main cause is that the temperature & concentration fields decreases as the kr rises due to thermal conductivity of the particles in the liquid decrease and an upsurge in the number of solute molecules participating in the reaction. Therefore, a harmful chemical reaction greatly declines the thickness of the thermal & concentration frontier stratum.

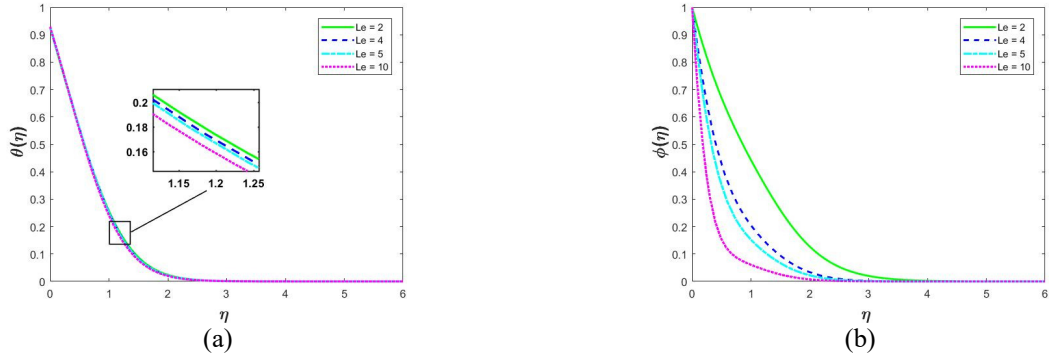

Figure 11. Impact of Le on (a) Temperature (b) Concentration

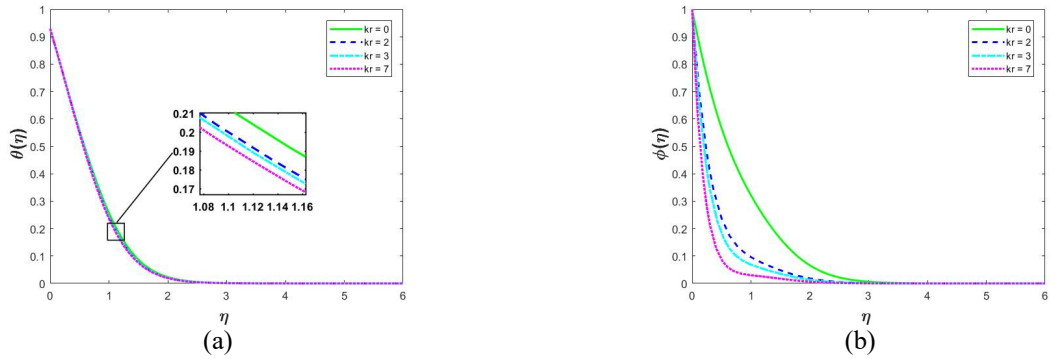

Figure 12. Impact of Kr on (a) Temperature (b) Concentration

The Fig 13. shows the variation of skin friction, Nusselt and Sherwood number with the variation of suction, velocity slip, stretching, magnetic and Casson parameter. Skin friction increases as enhancing of suction, stretching, magnetic and Casson parameter while decreasing as enhancing of velocity slip quantity. Amount of heat transfer improve as enhancing the suction parameter while fall down as enhancing of stretching, velocity slip, magnetic and Casson parameter. Amount of mass transmission raising as suction, stretching parameter while decreasing as enhancing of velocity slip, magnetic and Casson parameter. The Fig 14. Shows the variation of Nusselt & Sherwood number. Proportion of heat transmission enhancing as growing of thermal radiation and surface temperature while decreasing as enhancing chemical reaction and thermal slip quantities. Rate of mass transfer raising as enhancing of chemical reaction, thermal slip, thermal radiation while decreasing as enhancing of surface temperature parameter.

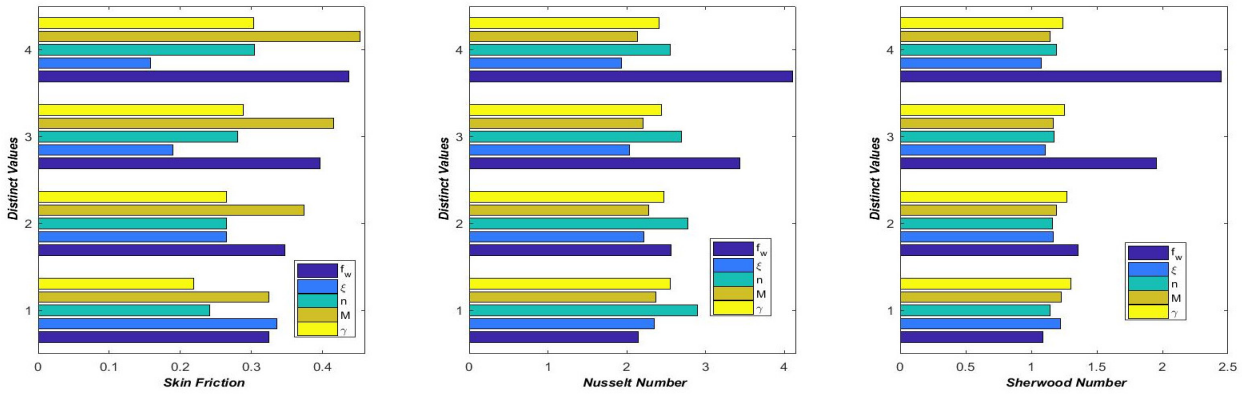

Figure 13. Skin frication, Nusselt and Sherwood number variation with the impact of f_w, ξ, n, M, γ

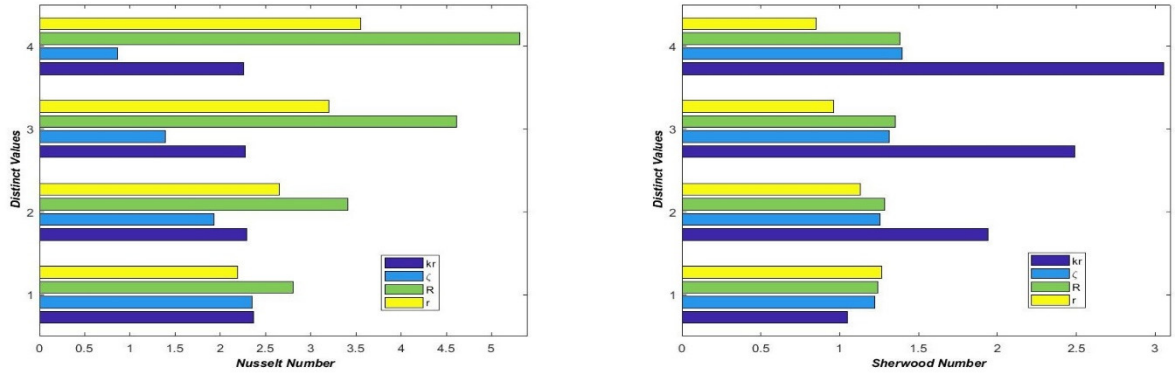

Figure 14. Nusselt and Sherwood number variation with the impact of kr, ζ, R, r

CONCLUSIONS

The purpose of the numerical study is to examine the effect of thermal radiation across a non-linear extending sheet on MHD Casson nano fluid. To solve the resulting ODEs with frontier circumstances and parameter modifications, the numerical schema bvp4c is used. The subsequent decisions are obtained.

- As the Casson, Magnetic parameter, and Prandtl number increase, the fluid's viscosity and that of the thermal frontier stratum decline.
- Lewis number and Brownian diffusion's effects, which are related to the temperature & concentration of reversible fluid flow.
- The temperature & concentration profiles rise with increasing velocity slip value.
- As the thermal slip parameter enhances, the thickness of the thermal frontier stratum falls.
- Temperature of the nanofluid increases while concentration of the fluid decreases with enhancement of the radiation parameter
- Decreases the thickness of the thermal & concentration frontier stratum by enhancing of Chemical decomposition rate.
- Skin friction raises as enhancing of suction, stretching, magnetic and Casson parameter while decreasing as enhancing of velocity slip quantity.
- Rate of heat transfer enhancing as increasing of thermal radiation and surface temperature while decreasing as enhancing chemical reaction and thermal slip quantities.
- Rate of mass transfer raising as enhancing of chemical reaction, thermal slip, thermal radiation while decreasing as enhancing of surface temperature parameter.

- The present results are in good agreement with earlier existed results.
- After discovering all the aforementioned results, we can determine that in several cases industrial production where the surfaces are stretching. Polymer sector when subjected to an external transverse magnetic field effect of several factors. The temperature and density of nanoparticles directly impact the quality of the material. Improving the final product can be achieved by controlling these factors at the period of manufacturing.

ORCID

P. Raja Shekar, https://orcid.org/0000-0003-4028-4688; **G. Jithender Reddy,** https://orcid.org/0000-0002-0103-1146
N. Pothanna, https://orcid.org/0000-0003-3983-3125

REFERENCES

[1] B.C. Sakiadis, "Boundary-layer behaviour on continuous solid surfaces: II. The boundary-layer on a continuous flat surface," AICHE J. 7**, (**1961). https://doi.org/10.1002/aic.690070211
[2] E.M.A. Elbashbeshy, and M.A.A Bazid, "Heat transfer over an unsteady stretching surface with internal heat generation," Appl. Math. Comput. **138**(2), (2003). https://doi.org/10.1016/S0096-3003(02)00106-6
[3] L.J. Crane, "Flow past a stretching plate," Journal of Applied Mathematics and Physics, **21**, (1970). https://doi.org/10.1007/BF01587695
[4] Z. Abbas, S. Rasool, and M. M. Rashidi, "Heat transfer analysis due to an unsteady stretching/shrinking cylinder with partial slip condition and suction," Ain Shams. Eng. J. **6,** (2015). https://doi.org/10.1016/j.asej.2015.01.004
[5] A.V. Rosca, N.C. Rosca, and I. Pop, "Numerical simulation of the stagnation point flow past a permeable stretching/shrinking sheet with convective boundary condition and heat generation," Internat. J. Numer. Methods Heat Fluid Flow, **26,** (2016). http://dx.doi.org/10.1108/HFF-12-2014-0361
[6] S.U. Choi, and J.A. Eastman, in: *Enhancing Thermal Conductivity of Fluids with Nanoparticles*, (Argonne National Lab., IL, United States, 1995), 12. (No. ANL/MSD/ CP-84938; CONF-951135-29).
[7] K. Das, T. Chakraborty, and P. Kumar Kundu, "Slip effects on nanofluid flow over a nonlinear permeable stretching surface with chemical reaction," Proceedings of the Institution of Mechanical Engineers, Part C: Journal of Mechanical Engineering Science. **230**(14), 2473 (2016). https://doi.org/10.1177/0954406215595654
[8] T. Hayat, M.W. Ahmad, S.A. Khan, and A. Alsaedi, "Computational treatment of statistical declaration probable error for flow of nanomaterials with irreversibility," Adv. Mech. Eng. **14,** (2022). https://doi.org/10.1177/16878140211070
[9] J. Wang, Y.P. Xu, R. Qahiti, M. Jafaryar, M.A. Alazwari, N.H. Abu-Hamdeh, and M.M. Selim, "Simulation of hybrid nanofluid flow within a microchannel heat sink considering porous media analyzing CPU stability," J. Petrol. Sci. Eng. **208,** 109734 (2022). http://dx.doi.org/10.1016/j.petrol.2021.109734
[10] W.A. Khan, and I. Pop, "Boundary-layer flow of a nanofluid past a stretching sheet," International Journal of Heat and Mass Transfer, **53,** 2477 (2010). https://doi.org/10.1016/j.ijheatmasstransfer.2010.01.032
[11] M.M. Rahman, and I.A. Eltayeb, "Radiative heat transfer in a hydromagnetic nanofluid past a non-linear stretching surface with convective boundary condition," Meccanica, **48**, 601 (2013). https://doi.org/10.1007/s11012-012-9618-2
[12] Md.T. Sk, K. Das, and P.K. Kundu, "Effect of magnetic field on slip flow of nanofluid induced by a non-linear permeable stretching surface," Applied Thermal Engineering, **104,** 758 (2016). http://dx.doi.org/10.1016/j.applthermaleng.2018.02.089
[13] Mahantesh M. Nandeppanavar, M.C. Kemparaju, and S. Shakunthala, "MHD stagnation point slip flow due to a non-linearly moving surface with effect of non-uniform heat source," Nonlinear Eng. **8,** 270 (2019). http://dx.doi.org/10.1515/nleng-2017-0109
[14] N. Vedavathi, G. Dharmaiah, K.S. Balamurugan, and J. Prakash, "Heat transfer on MHD nanofluid flow over a semi-infinite flat plate embedded in a porous medium with radiation absorption, heat source and diffusion thermo effect," Frontiers in Heat and Mass Transfer, **9,** 38 (2017). https://doi.org/10.5098/hmt.9.38
[15] P. Biswas, S.M. Arifuzzaman, M. Rahman, and M.S. Khan, "Effects of periodic magnetic field on 2D transient optically dense gray nanofluid over a vertical plate: a computational EFDM study with SCA," Journal of Nanofluids, **7**(1), 82 (2018). https://doi.org/10.1166/jon.2018.1434
[16] O.A. Beg, M.S. Khan, I. Karim, M.M. Alam, and M. Ferdows, "Explicit numerical study of unsteady hydromagnetic mixed convective nanofluid flow from an exponentially stretching sheet in porous media," Appl. Nano. sci. **4**, 943 (2014). http://dx.doi.org/10.1007/s13204-013-0275-0
[17] Al-Mamun, S.M. Arifuzzaman, S. Reza-E-Rabbi, P. Biswas, and M.S. Khan, "Computational modelling on MHD radiative Sisko nanofluids flow through a nonlinearly stretching sheet," International Journal of Heat and Technology, **37**(1), 285 (2019). http://dx.doi.org/10.18280/ijht.370134
[18] G. Dharmaiah, W. Sridhar, K.S. Balamurugan, and K.C. Kala, "Hall and ion slip impact on magneto-titanium alloy nano liquid with diffusion thermo and radiation absorption," Int. J. Ambient Energy, **43**, 3507 (2022). https://doi.org/10.1080/01430750.2020.1831597
[19] T.S.R.P. Roja, S.M. Ibrahim, M. Parvathi, G. Dharmaiah, and G. Lorenzini, "Magnetic field influence on Thermophoretic Micropolar fluid flow over an inclined permeable surface: a numerical study," J. Appl. Comput. Mech. **10**(2), 369 (2024). https://doi.org/10.22055/jacm.2024.44739.4265
[20] N. Casson, "A flow equation for pigment-oil suspensions of the printing ink type," Rheology of Disperse Systems, **84,** (1959).
[21] D.A. McDonald, *Blood flow in arteries.* 2nd ed. (Edward Arnold Ltd: Great Britain, 1974).
[22] P. Nagarani, V.M. Job, P.V.S.N. Murthy, "The effect of peristalsis on dispersion in Casson fluid flow," Ain Shams Engineering Journal, **15**, (2024). https://doi.org/10.1016/j.asej.2024.102758
[23] B.V. Awati, A. Goravar, N.M. Kumar, and G. Bognar, "Stability analysis of magnetohydrodynamic Casson fluid flow and heat transfer past an exponentially shrinking surface by spectral approach," Case Studies in Thermal Engineering. **60,** 104810 (2024). https://doi.org/10.1016/j.csite.2024.104810

[24] N. Abbas, W. Shatanawi, and T.A.M. Shatnawi, "Thermodynamic properties of Casson-Sutterby-micropolar fluid flow over exponential stretching curved sheet with impact of MHD and heat generation," Case Studies in Thermal Engineering, **55**, (2024).
[25] B.N. Reddy, and P. Maddileti, "Casson nanofluid and Joule parameter effects on variable radiative flow of MHD stretching sheet," Partial Differential Equations in Applied Mathematics. **7**, 100487 (2023). https://doi.org/10.1016/j.padiff.2022.100487
[26] B.P. Reddy, P.M. Matao, and J.M. Sunzu, "A finite difference study of radiative mixed convection MHD heat propagating Casson fluid past an accelerating porous plate including viscous dissipation and Joule heating effects," Heliyon, **10**, e28591 (2024). https://doi.org/10.1016/j.heliyon.2024.e28591
[27] Y.D. Reddy, and B.S. Goud, "Comprehensive analysis of thermal radiation impact on an unsteady MHD nanofluid flow across an infinite vertical flat plate with ramped temperature with heat consumption," **17**, 100796 (2023). https://doi.org/10.1016/j.rineng.2022.100796
[28] N.A. Zainal, R. Nazar, K. Naganthran, and I. Pop, "The Impact of Thermal Radiation on Maxwell Hybrid Nanofluids in the Stagnation Region," Nanomaterials (Basel), **12**(7), 1109 (2022). https://doi.org/10.3390/nano12071109
[29] A.M.A. Alrashdi, "Mixed convection and thermal radiation effects on non-Newtonian nanofluid flow with peristalsis and Ohmic heating," Front. Mater. **10**, 1178518 (2023). https://doi.org/10.3389/fmats.2023.1178518
[30] A.M. Rashad, M.A. Nafe, and D.A. Eisa, "Heat Generation and Thermal Radiation Impacts on Flow of Magnetic Eyring–Powell Hybrid Nanofluid in a Porous Medium," Arab. J. Sci. Eng. **48**, 939 (2023). https://doi.org/10.1007/s13369-022-07210-9
[31] Y.P. Lv, N. Shaheen, M. Ramzan, *et al*., "Chemical reaction and thermal radiation impact on a nanofluid flow in a rotating channel with Hall current," Sci. Rep. **11**, 19747 (2021). https://doi.org/10.1038/s41598-021-99214-y
[32] S. Arulmozhi, K. Sukkiramathi, S.S. Santra, R. Edwan, U. Fernandez-Gamiz, and S. Noeiaghdam, "Heat and mass transfer analysis of radiative and chemical reactive effects on MHD nanofluid over an infinite moving vertical plate," Results in Engineering, **14**, 100394 (2022). https://doi.org/10.1016/j.rineng.2022.100394
[33] B.H. Athal, A. Sasikala, B.N. Reddy, V. Govindan, P. Maddileti, K. Saritha, B.S. Reddy, *et al*., "Combined impact of radiation and chemical reaction on MHD hyperbolic tangent nanofluid boundary layer flow past a stretching sheet," Modern Physics Letters B, **38**(16), 2341010 (2024). https://doi.org/10.1142/S0217984923410105
[34] A.M. Sedki, "Effect of thermal radiation and chemical reaction on MHD mixed convective heat and mass transfer in nanofluid flow due to nonlinear stretching surface through porous medium," Results in Materials, **16**, 100334 (2022). https://doi.org/10.1016/j.rinma.2022.100334
[35] M. Eid, and O.D. Makinde, "Solar radiation effect on a magneto nanofluid flow in a porous medium with chemically reactive species," Int. J. Chem. React. Eng. **16**(9), 2017012 (2018). http://dx.doi.org/10.1515/ijcre-2017-0212
[36] N.T.M. Eldabe, A.Y. Ghaly, M.A.A. Mohamed, and M.S.H. Mohamoud, "MHD boundary layer chemical reacting flow with heat transfer of Eyring -Powell nanofluid past a stretching sheet," Microsyst. Technol. **24**, 4945 (2018). https://doi.org/10.1007/s00542-018-3915-1
[37] B.J. Gireesha, and N.G. Rudraswamy, "Chemical reaction on MHD flow and heat transfer of a nanofluid near the stagnation point over a permeable stretching surface with non-uniform heat source/sink," International Journal of Engineering, Science and Technology, **6(5)**, 13 (2014). https://doi.org/10.4314/ijest.v6i5.2
[38] A.Bhandari, "Radiation and Chemical Reaction Effects on Nanofluid Flow Over a Stretching Sheet," Fluid Dynamics & Materials Processing, **15**(5), 557 (2019). https://doi.org/10.32604/fdmp.2019.04108
[39] W. Jamshed, V. Kumar, and V. Kumar, "Computational examination of Casson nanofluid due to a non- linear stretching sheet subjected to particle shape factor: Tiwari and Das model," Numerical Methods for Partial Differential Equations **38**(4), 848 (2022). https://doi.org/10.1002/num.22705
[40] I. Ullah, K.S. Nisar, S. Shafie, I. Khan, M. Qasim, and A. Khan, "Unsteady free convection flow of Casson nanofluid over a nonlinear stretching sheet," IEEE Access, **7**, 93076 (2019). https://doi.org/10.1109/access.2019.2920243

ВПЛИВ ТЕПЛОВОГО ВИПРОМІНЮВАННЯ НА МГД ПОТІК НАНОРІДИНИ КАССОНА ЧЕРЕЗ ЛИСТ ЩО НЕЛІНІЙНО РОЗТЯГУЄТЬСЯ З НАЯВНОСТЮ ХІМІЧНОЇ РЕАКЦІЇ

П. Раджа Шекар, Г. Джитендер Редді, Н. Потанна

Кафедра математики, Інженерно-технологічний інститут VNR Віньяна Джьоті, Хайдарабад, 500090, Телангана, Індія

Метою цього дослідження є вивчення впливу параметра Кассона та хімічної реакції на змінний радіаційний МГД потік нанофлюїду через лист, що розтягується. Завдяки використанню функцій подібності рівняння моделювання (PDE) руху рідини перетворюються на прості диференціальні рівняння. Інструмент MATLAB використовується для чисельного обчислення рівнянь. Графіки та описи надані для контурів швидкості, концентрації та температури, що показують вплив важливих обмежень потоку рідини. Аналізуються різні фактори, щоб отримати дані та пояснення чисел Прандтля, Льюїса, параметрів ковзання та хімічного розкладання. Поточні результати є хорошими та добре узгоджуються з наявними звітами. В'язкість флюїду та термічного граничного шару зменшується зі збільшенням Кассона, магнітного параметра та числа Прандтля. Поверхневе тертя збільшується при збільшенні всмоктування, розтягування, магнітного параметра та параметра Кассона, а також зменшується через збільшення швидкісного ковзання. Швидкість передачі тепла збільшується у міру збільшення теплового випромінювання та температури поверхні, одночасно зменшуючись у міру посилення хімічної реакції та теплового ковзання. Швидкість масообміну підвищується за рахунок посилення хімічної реакції, теплового ковзання, теплового випромінювання та зменшується за рахунок збільшення параметра температури поверхні.

Ключові слова: *нанофлюїд; хімічна реакція; термофорез; броунівський рух*